

<http://ansinet.com/itj>

ITJ

ISSN 1812-5638

INFORMATION TECHNOLOGY JOURNAL

ANSI*net*

Asian Network for Scientific Information
308 Lasani Town, Sargodha Road, Faisalabad - Pakistan

A Novel Lightness Localization Algorithm in Wireless Sensor Networks Based on Anchor Nodes Equilateral Triangle Layout

Ai Jiang-Shan and Chen Xiao-Hong
Business School of Central South University, Hunan, Changsha, China

Abstract: In this study we propose a new Lightness Equilateral Triangle Localization Algorithm (LETLA) that accurately localizes sensors while minimizing power consumption and independent on any extra hardware. In the LETLA, which is based on geometric characteristics of equilateral triangle layout, anchors are placed in the vertexes of many equilateral triangles. The equilateral triangle that contains the located node is determined by examining the ordered sequence of ranging result taken at multiple anchor nodes and the intersection of two arcs is substituted by the intersection of two tangent lines which is the approximate location of located point in LETLA. Through extensive simulations, we show that LETLA performs better than other state of the art approaches in terms of energy consumption with the same localization precision.

Key words: WSNs, equilateral triangle layout, localization

INTRODUCTION

Wireless Sensor Network (WSN) has become popular due to its wide applicability (Mainwaring *et al.*, 2002; Yang and Wang, 2007; Wang *et al.*, 2007; Wang *et al.*, 2008; Qian *et al.*, 2007;). Therefore knowledge of the node positions used to detect and record events and to route packets using geometric-aware routing becomes imperative (Younis *et al.*, 2006; Baggio and Langendoen, 2008; Niculescu and Nath, 2003). Power consumption is a big challenge in WSN because sensors have limited power but many localization methods in WSN consume a mass of energy in complex arithmetic operations to improve localization precision (Zhou *et al.*, 2008; Wang and Jin, 2009; Li *et al.*, 2009; Ampeliotis and Berberidis, 2010).

In this study we introduce a Lightness Equilateral Triangle Localization Algorithm (LETLA) that achieves good accuracy relative to up-to-date localization algorithms while minimizing power consumption. We consider a network has a layout in which all the anchors are placed in the vertexes of many identical equilateral triangles that cover the location area completely. The order of ranging results is identical to the distance order based on true euclidean distances. In our approach the located node is restricted to lie in some equilateral triangle called target equilateral triangle which determined by the order of ranging results. The coordinate of located node, according to the principle of triangulation in the target equilateral triangle, is the coordinate of intersection of two arcs. The center and radius of arc are the anchor in the vertex of target equilateral triangle or the adjacent

equilateral triangle and the ranging result taken at the center of arc.

The key idea of our localization algorithm is that the intersection of two arcs is substituted by the intersection of two tangent lines, which losses less accuracy and saves more energy consumption. In the following a principle of choosing the point of tangency which is an optimization problem to minimize the approximate substitute error in converting arc into tangent line is presented and geometric characteristics of equilateral triangle layout that has been utilized in a method to achieve the better localization precision is described.

This study is organized as follows. In section 2, the Lightness Equilateral Triangle Localization Algorithm (LETLA) method is given. In section 3, the geometric characteristics of equilateral triangle layout is described. In section 4, the principle of determining point of tangency is presented. The experimental results of comparing the localization algorithm proposed in this study with other localization algorithms are also presented in section 5. Finally, our work of this study is summarized in the last section.

LETLA METHOD

In this section, we present LETLA method and illustrate it through examples. Assume that a 2D localization space consists of n anchors and the located node P knows the coordinate of every anchor. The objective of localization is calculating the coordinate of node P with the range results of anchors and the layout of the anchors. All the anchors are placed in the vertexes of

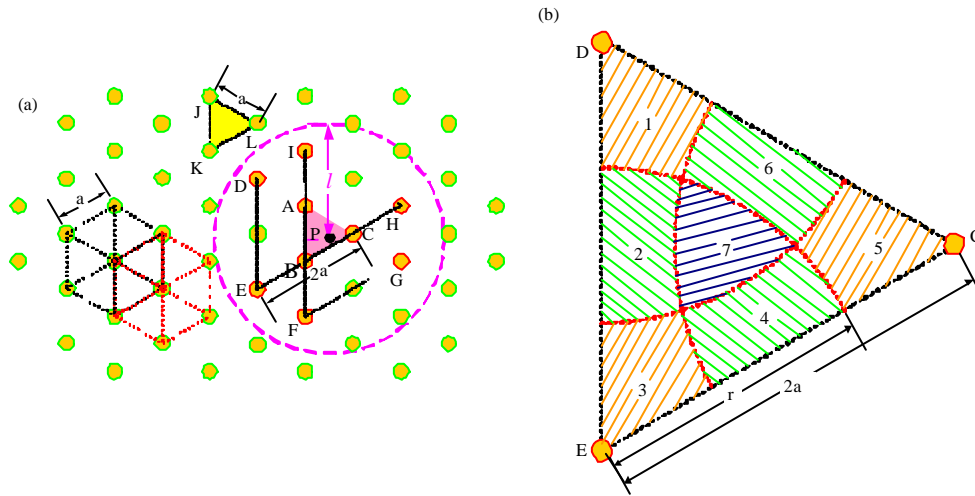


Fig. 1(a-b). Anchors' Layout and Division of DEC

many identical equilateral triangles that cover the location area completely, as shown in Fig. 1a. Each anchor is encircled by its six neighbor anchors with same distance represented by letter a and the radio range of anchors and located node P is represented by letter l that satisfies Eq. 1.

$$l \geq 2a \quad (1)$$

The procedure for localization of unknown nodes using LETLA method is given as follows:

Step 1: Figure 1a shows the located node P measures the distance of 9 anchors by some range technique as TDOA, AOA, TOA and RSSI. The 9 anchors are anchor A, B, C, D, E, F, G, H and I , which satisfy a geometric constraint illustrated in Fig. 1a. The order of 9 distances between node P and 9 anchors determine the equilateral triangle named target equilateral triangle, which contains node P . The anchors on the 3 vertexes of target equilateral triangle are the 3 nearest anchors, because the order of ranging results are identical to the distance order based on true euclidean distances in the anchors equilateral triangle layout. ABC is the target equilateral triangle in Fig. 1a as anchor A, B and C has the less ranging result than any other anchors (Δ is a symbol of equilateral triangle).

Step 2: Based on the result of former processing step, node P is in ΔABC and the order and value of 9 ranging results of anchors in the vertexes of $\Delta DEC, \Delta IBH$ and ΔAFG between node P are known. Taking anchor nodes equilateral triangle layout into account, $\Delta DEC, \Delta IBH$ and

ΔAFG have advantages on localization as ΔABC is the target Δ . Each of $\Delta DEC, \Delta IBH$ and ΔAFG is divided into seven distinct regions by 3 arcs which are composed of anchors in the vertex of equilateral triangle and radius represented by letter r . Figure 1b shows an instance of the division in ΔDEC and anchor D, E and C are the centers of 3 arcs with the radius of r . The above procedure opens itself to the following questions: Why the each of $\Delta DEC, \Delta IBH$ and ΔAFG is divided into seven distinct regions? How to determine the length of r ? In section 3, we answer the above questions.

Step 3: As illustrated in Fig. 2a, located node P is in the position of the intersection of two arcs in target ΔABC . One centered at the anchor C with radius of the distance between anchor C and P in ΔDEC and the other one centered at the anchor F with radius of the distance between anchor F and P in ΔAFG . We substitute the intersection of two tangencies for the intersection of two arcs, since the solution of tangential equations has less computational complexity than the solution of arc equations. Fig. 2b shows the coordinate of Q solved by the tangential equations close to the coordinate of located node P solved by the arc equations, which benefits from a reasonable option of point of tangency on arc and a rational choice of arcs to calculate the intersection by the target Δ determination and the regions containing located node P in $\Delta DEC, \Delta IBH$ and ΔAFG . The principle of choosing the point of tangency in arc is described in section 4.

The localization can be summarized as follow. (1) Node P ranges distances between all the anchors and

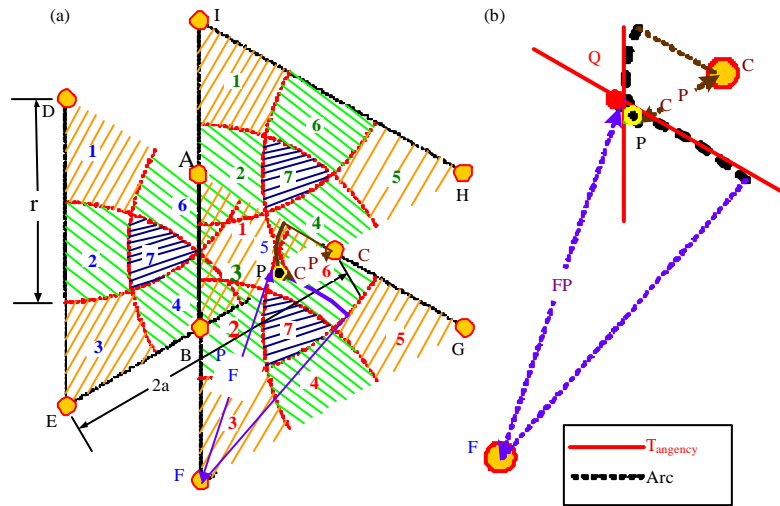


Fig. 2(a-b): (a) P is in the intersection of two arcs and (b) Q is an approximate coordinate of located node P

selects the 3 nearest anchors according the ranging results to determine the 3 vertexes of target Δ which can be determine simultaneously. As shown in Fig. 1a, ΔABC is the target Δ , because anchor A, B and C have the least distance between node P. (2) The 3 Δ with $2a$ side can be determined by the character that is the union area of 3 Δ is target Δ . As illustrated in Fig. 1a, ΔDEC , ΔIBH and ΔAFG are the objectives, since target ΔABC their union area. For optimizing the approximate error in step 3, each of 3 Δ is divided into 7 regions. Figure 1b is an example of ΔDEC . (3) The intersection of two arcs whose centers are in the vertexes of 3 Δ determined in step 2 is substituted for the intersection of two tangencies as shown in Fig. 2. The computation complexity decreases sharply benefited from the approach in step 3 and localization accuracy is still in a high level.

GEOMETRIC CHARACTERISTICS OF EQUILATERAL TRIANGLE LAYOUT

In this section, we present the reason of dividing ΔDEC , ΔIBH and ΔAFG and the means of computing value of r . For minimizing the approximate error, when the intersection of two arcs is substituted by the intersection of two tangencies, we introduce a conclusion that states approximate error is proportional to central angles and radii of arcs is proved in section 4. The division in ΔDEC , ΔIBH and ΔAFG are used to solve a multi-objective constrained optimum problem of minimizing the central angles and radii of arcs simultaneously.

As shown in Fig. 3a, the central angles of arcs are 60° and the radii of arcs range is $[0, 2a]$ in ΔDEC which is regard as a whole, when the vertexes of ΔDEC are the

centers of arcs. If there are 7 regions in ΔDEC , the arcs in different regions have different central angles and different radii. Figure 3 (a) shows the central angles of arcs in region 2, 4, 6 and 7 are less than 30° and radii of arcs in region 1, 3 and 5 is $[0, 1.3a]$. Dividing ΔDEC gets better approximate performance than regarding ΔDEC as a whole for less central angles and radii of arcs, because of the conclusion that states approximate error is directly proportional to central angles and radii of arcs.

By using cosine law in ΔDEC as shown in Fig. 3b, we introduce Eq. 2 to obtain the expression of r , where r is the radius of arc used to divide ΔDEC to 7 regions and a is the distance of two neighbor anchors:

$$r^2 = (2a)^2 + \left(\frac{\sqrt{3}}{2}a\right)^2 - 2 \times 2a \times \frac{\sqrt{3}}{2}a \times \cos\left(\frac{\pi}{6}\right) \tag{2}$$

The value of r is given by Eq. 3 expressed in a function of variable a :

$$r = \frac{\sqrt{7}}{2}a \tag{3}$$

PRINCIPLE OF DETERMINING POINT OF TANGENCY

The number of tangency on an arc is infinite as the number of point of tangency on an arc is infinite. This section focuses on the research on how to determine the point of tangency on an arc for minimizing approximate error of substituting the intersection of two arcs for the intersection of two tangencies.

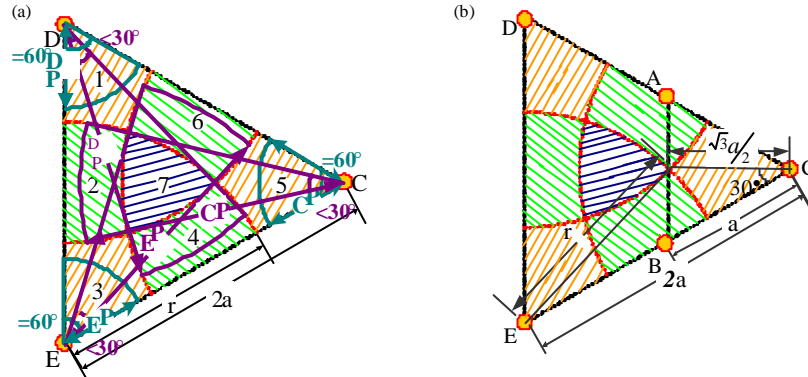


Fig. 3(a-b): (a) Division in $\triangle DEC$ makes central angles and radii of arcs reduced to get better approximation of substituting the intersection of two tangencies for the intersection of two arcs and (b) Approach of determining the length of r

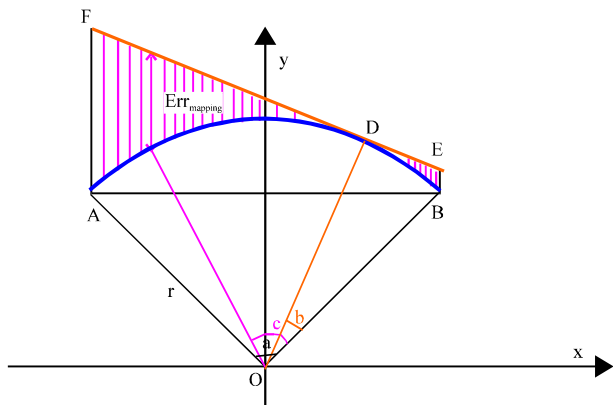


Fig. 4: Definition Of ermapping

As shown in Fig. 4, an arc AB is approximated to a tangency FE. The central angle and radius of AB are expressed by a and r and the center of AB is the origin of coordinate system in which Y axis bisects AB. The coordinate of point on AB is expressed by (x_{arc}, y_{arc}) and $(x_{tangent}, y_{tangent})$ express the coordinate of point on FE. $Err_{mapping}$ is a symbol of approximate error and defined in Eq. 4:

$$Err_{mapping} = y_{tangent} - y_{arc} \quad (x_{tangent} = x_{arc}) \quad (4)$$

Assume point D is the position of point of tangency of FE and also a point on AB, determining the position of point D on AB is equated determining the degree of angle b in range of [0, a]. When the position of point D is given through determining degree of angle b,

there is an infinite number of $Err_{mapping}$ in Fig. 4, because each coordinate on the X axis correspond to an $Err_{mapping}$. By using an angle c, coordinate on the X axis and Y axis can be constructed in Eq. 3 and 5-7:

$$x_{tangent} = x_{arc} = r \times \cos\left(\frac{\pi}{2} + c - \frac{a}{2}\right) \quad (5)$$

$$y_{tangent} = r \times \tan\left(\pi - \frac{a}{2} + b\right) \times \left[\sin\left(\frac{a}{2} - c\right) - \sin\left(\frac{a}{2} - b\right)\right] + r \times \cos\left(\frac{a}{2} - b\right) \quad (6)$$

$$y_{arc} = r \times \sin\left(\frac{\pi}{2} - \frac{a}{2} + c\right) = r \times \cos\left(\frac{a}{2} - c\right) \quad (7)$$

For demands of optimizing $Err_{mapping}$ the expression for can be given in Eq. 8 combined Eq. 4-7 in a function of angle a, b and c:

$$Err_{mapping} = r \times \left(\frac{1 - \cos(b-c)}{\cos\left(\frac{a}{2} - b\right)}\right) \quad (8)$$

Angle a is the central angle of AB, which is given with the arc. Angle b is the angle depends on the position of point of tangency, which is known as the point of tangency D is determined. If arc AB and tangency FE are given, angle a and b are constants and angle c is variable with a range of [0, a] corresponding to all the $Err_{mapping}$ in the area between arc and tangency in Fig. 4.

The next step is to establish 3 functions E ($Err_{mapping}$), D ($Err_{mapping}$) and Max ($Err_{mapping}$) that describes $Err_{mapping}$ from statistics.

$E(\text{Err}_{\text{mapping}})$ is the mean of $\text{Err}_{\text{mapping}}$ in the area between arc and tangency in Fig. 4 and defined in Eq. 9:

$$\begin{aligned} E(\text{Err}_{\text{mapping}}) &= \frac{1}{x_B - x_A} \int_{x_A}^{x_B} \text{Err}_{\text{mapping}} dx \\ &= \frac{r}{2 \sin(\frac{a}{2})} \left[\frac{8 \sin(\frac{a}{2}) - \sin(\frac{3}{2}a - b) - \sin(\frac{a}{2} + b)}{4 \cos(\frac{a}{2} - b)} - \frac{a}{2} \right] \end{aligned} \quad (9)$$

where, $D(\text{Err}_{\text{mapping}})$ is the variance of $\text{Err}_{\text{mapping}}$ in the area between arc and tangency in Fig. 4 and defined in Eq. 10:

$$\begin{aligned} D(\text{Err}_{\text{mapping}}) &= \frac{1}{x_B - x_A} \int_{x_A}^{x_B} (\text{Err}_{\text{mapping}} - E(\text{Err}_{\text{mapping}}))^2 dx \\ &= \frac{1}{2 \sin(\frac{a}{2})} \int_0^a (\text{Err}_{\text{mapping}} - E(\text{Err}_{\text{mapping}}))^2 \times \cos(\frac{a}{2} - c) dc \end{aligned} \quad (10)$$

$\text{Max}(\text{Err}_{\text{mapping}})$ is the maximum of $\text{Err}_{\text{mapping}}$ in the area between arc and tangency in Fig. 4 and defined in Eq. 11.

$$\text{Max}(\text{Err}_{\text{mapping}}) = \begin{cases} r \times \left(\frac{1 - \cos(a-b)}{\cos(\frac{a}{2} - b)} \right), & 0 \leq b < \frac{a}{2}, \quad c = a \\ r \times \left(\frac{1 - \cos(\frac{a}{2})}{1} \right), & b = \frac{a}{2}, \quad c = 0 \quad \text{or} \quad c = a \\ r \times \left(\frac{1 - \cos(b)}{\cos(\frac{a}{2} - b)} \right), & \frac{a}{2} \leq b < a, \quad c = 0 \end{cases} \quad (11)$$

The object of this section is to find the position of point of tangency D that minimizes the value of $E(\text{Err}_{\text{mapping}})$, $D(\text{Err}_{\text{mapping}})$ and $\text{Max}(\text{Err}_{\text{mapping}})$. As the position of point of tangency D can be constructed in angle b, the object is converted to determine angle b to minimize the value of $E(\text{Err}_{\text{mapping}})$, $D(\text{Err}_{\text{mapping}})$ and $\text{Max}(\text{Err}_{\text{mapping}})$.

The solution of equations, established by the first derivative of $E(\text{Err}_{\text{mapping}})$ and $D(\text{Err}_{\text{mapping}})$ equal zero, can be expressed by $b = 0.5a$ that indicates $b = 0.5a$ is the way to minimize $E(\text{Err}_{\text{mapping}})$ and $D(\text{Err}_{\text{mapping}})$. It can proved $b = 0.5a$ is also the way to minimize $\text{Max}(\text{Err}_{\text{mapping}})$, by calculating the maximum of $\text{Err}_{\text{mapping}}$ as angle b ranging from $[0, a]$.

By summarizing the analysis in this section, the values of $E(\text{Err}_{\text{mapping}})$, $D(\text{Err}_{\text{mapping}})$ and $\text{Max}(\text{Err}_{\text{mapping}})$ is the least value when angle b equals $0.5a$. It denotes the position of point of tangency D is the median point of arc AB, which minimizes the mean, variance and maximum of $\text{Err}_{\text{mapping}}$. Because $\text{Err}_{\text{mapping}}$ is a representation of approximate error, minimizing $E(\text{Err}_{\text{mapping}})$, $D(\text{Err}_{\text{mapping}})$ and

$\text{Max}(\text{Err}_{\text{mapping}})$ can reduce approximate error. Therefore we choose the median point of arc to be the position of point of tangency mentioned in step 3 of section 1.

EXPERIMENTAL RESULT

Localization error are calculated in target ΔABC with $a = 50$ m in Fig. 1a. Localization error is defined in term of the euclidean distance between the coordinate computed by LETLA and the coordinate of the true position. Located node P is in ΔABC , since ΔABC is target Δ . Every point in ΔABC has a corresponding localization error. Figure 5 shows localization error in ΔABC in which X and Y axis indicate the position of located node P in ΔABC and Z axis expresses the value of localization error. The percentage of area in ΔABC in which localization error less than 1m is 72.971% and the percentage of area in ΔABC in which localization error less than 3 m is 90.519%. The maximum and minimum of localization error in ΔABC is 0 m and 6.13 m.

The evaluation is performed through simulations by using the NS-2 simulator to compare four localizations LETLA proposed in this study, Voronoi Diagrams Localization¹², Weighted Centroid Localization¹³ and Sequence-Based Localization¹⁴. The simulation parameters are based on the MicaZ sensor node. The communication range is fixed in 50 m for all nodes and localization area is a square of 100×100 m. The default parameters for the experiments are presented in Table 1. We record the localization error and computing energy in 60 independent experiments. The averages of these values are shown in Fig. 5-7.

The distribution of localization errors among the noise variance is depicted in Fig. 6. As can be seen, when the value of noise variance increases, the localization error of 4 localizations increases at the same time. A gentle curve means that the localization has an anti-noise ability. As shown in Fig. 6, the best results are achieved by LETLA algorithms where cave increases slowly and less than the other 3 algorithms. This suggests that anti-noise ability of localization may have been significantly

Table 1: Simulation parameters in NS2

Parameter	Value
Channel bandwidth (kbps)	250
Frequency (GHz)	2.4
Wireless model	Shadowing
Pathloss	3
MAC protocol	IEEE802.15.4
Power for transmission (Watt)	0.28183815
Power for idle (Watt)	0.003587
Power for reception (Watt)	0.2182837
RX thresh (Watt)	1.35685e-11
RF radius (m)	50
Initial energy (J)	10

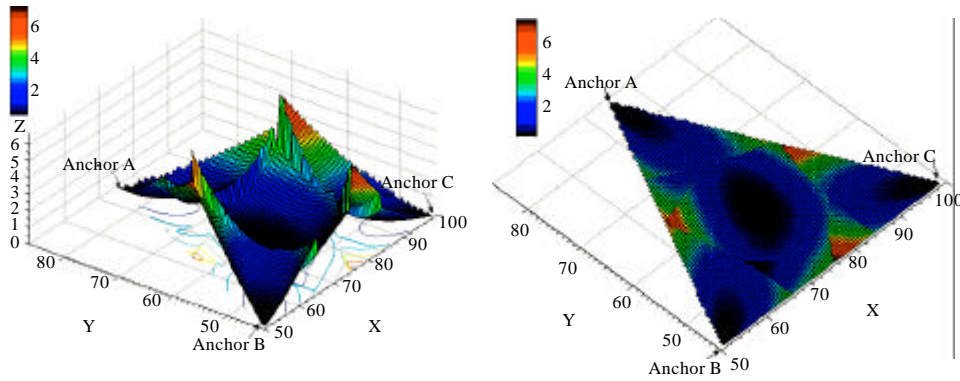


Fig. 5(a-b): (a) Side elevation of localization error in ABC and (b) Planform of localization error

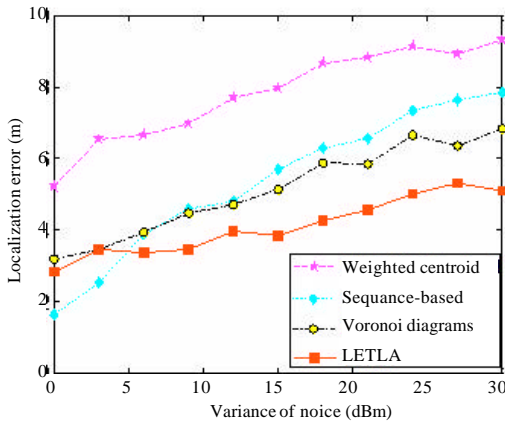


Fig. 6: Localization error VS variance of noise

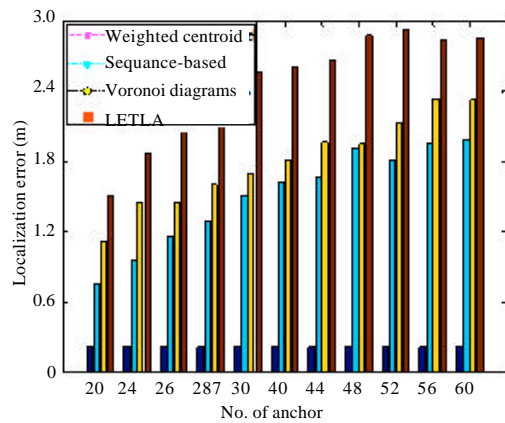


Fig. 8: Energy consumption VS number of anchor

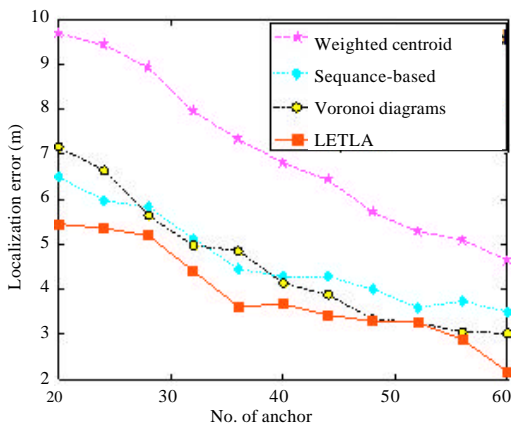


Fig. 7: Localization error VS number of anchor

error of LETLA is less than the other 3 localization on every point of X axis and it continues decreasing (more

promoted by using LETLA. This is because the geometric restriction of anchor nodes equilateral triangle layout is fixed and target Δ has better robustness than the method of point estimation and interval estimation used in Voronoi Diagrams Localization, Weighted Centroid Localization and Sequence-Based Localization.

Figure 7 depicts the localization error of 4 localizations when the number of anchors increases. As we can see, by increasing the number of anchors, we can reduce the localization error. Particularly, the localization sharply) with the increasing number of anchors. In other words, LETLA has the better performance of localization at the same number of anchors. It reveals that approximate error introduced in substituting the intersection of two arcs for the intersection of two tangencies is reasonable approach to reduce computing energy and obtain a high localization precision.

Figure 8 compare the computing energy for all four localization techniques. As the results show, LETLA performance of energy consumption doesn't increase with

increasing the numbers of anchors and the energy consumption of LETLA is less than 10% in comparison with Voronoi Diagrams Localization, Weighted Centroid Localization and Sequence-Based Localization at the same number of anchors. The results suggest that the substitution of linear equations composed of tangencies for quadratic equations composed of arcs is effective manner to reduce energy consumption. Because linear equations doesn't need complex arithmetic operations and statistical estimation to get a unique solution, under the same condition of communication LETLA can get a high precision with the least calculation procedures than the other 3 localization.

CONCLUSIONS

We proposed an algorithm LETLA for node localization in wireless sensor networks, which is based on geometric characteristics of equilateral triangle topological layout. Both outperform 3 existing state-of-the-art algorithms in terms of localization accuracy and energy consumption low. In the same situations where the variance of noise is high, LETLA outperforms all other algorithms. In the future we would like to explore 3D LETLA algorithms. We plan to study the effect of regular tetrahedron in 3D localization which can be used for approximate purposes in a hypersurface localization technique.

ACKNOWLEDGMENTS

This study was supported by the innovation Research Group Science Fund of the National Natural Science Foundation of China (No.71221061)

REFERENCES

Ampeliotis, D. and K. Berberidis, 2010. Sorted order- κ voronoi diagrams for model-independent source localization in wireless sensor networks. *IEEE Trans. Signal Process.*, 58: 426-437.

Baggio, A. and K. Langendoen, 2008. Monte Carlo localization for mobile wireless sensor networks. *Ad Hoc Networks*, 6: 718-733.

Li, X.Q., H. Gao and L.L. Lv, 2009. An improved APIT algorithm based on direction searching. *Proceedings of the 5th International Conference on Wireless Communications Networking and Mobile Computing*, September 24-26, 2009, Beijing, China, pp: 1-4.

Mainwaring, A., J. Polastre, R. Szewczyk, D. Culler and J. Anderson, 2002. Wireless sensor networks for habitat monitoring. *Proceedings of the 1st ACM International Workshop on Wireless Sensor Networks and Applications*, September 28, 2002, New York, USA., pp: 88-97.

Niculescu, D. and B. Nath, 2003. DV based positioning in ad hoc networks. *Telecommun. Syst.*, 22: 267-280.

Qian, Y., K. Lu and D. Tipper, 2007. A design for secure and survivable wireless sensor networks. *IEEE Wireless Commun.*, 15: 30-37.

Wang, J.Z. and H.G. Jin, 2009. Improvement on APIT localization algorithms for wireless sensor networks. *Proceedings of the International Conference on Networks Security, Wireless Communications and Trusted Computing*, Volume 1, April 25-26, 2009, China, pp: 719-723.

Wang, W., V. Srinivasan, B. Wang and K.C. Chua, 2008. Coverage for target localization in wireless sensor networks. *IEEE Trans. Wireless Commun.*, 7: 667-676.

Wang, X., D. Bi, L. Ding and S. Wang, 2007. Agent collaborative target localization and classification in wireless sensor networks. *Sensors*, 7: 1359-1386.

Yang, Q. and Z.J. Wang, 2007. Study on localization algorithms for large scale wireless sensor network. *Transducer Microsyst. Technol.*, 26: 33-36.

Younis, M., K. Ghunman and M. Eltoweissy, 2006. Location-aware combinatorial key management scheme for clustered sensor networks. *IEEE Trans. Parallel Distrib. Syst.*, 17: 865-882.

Zhou, Y., X. Ao and S.X. Xia, 2008. An improved APIT node self-localization algorithm in WSN. *Proceedings of the 7th World Congress on Intelligent Control and Automation*, June 25-27, 2008, Chongqing, China, pp: 7582-758.